

RESEARCH NOTE

Open Access



olf413 an octopamine biogenesis pathway gene is required for axon growth and pathfinding during embryonic nervous system development in *Drosophila melanogaster*

Ravindrakumar Ramya¹, Chikkate Ramakrishnappa Venkatesh¹ and Baragur Venkatanarayanasetty Shyamala^{1*}

Abstract

Objective Neurotransmitters have been extensively studied as neural communication molecules. Genetic associations discovered, and indirect intervention studies in Humans and mammals have led to a general proposition that neurotransmitters have a role in structuring of neuronal network during development. *olf413* is a *Drosophila* gene annotated as coding for dopamine beta-monooxygenase enzyme with a predicted function in octopaminergic pathway. The biological function of this gene is very little worked out. In this study we investigate the requirement of *olf413* gene function for octopamine biogenesis and developmental patterning of embryonic nervous system.

Result In our study we have used the newly characterized neuronal specific allele *olf413*^{SG1.1}, and the gene disruption strain *olf413*^{M102014} to dissect out the function of *olf413*. *olf413* has an enhancer activity as depicted by reporter GFP expression, in the embryonic ventral nerve cord, peripheral nervous system and the somatic muscle bundles. Homozygous loss of function mutants show reduced levels of octopamine, and this finding supports the proposed function of the gene in octopamine biogenesis. Further, loss of function of *olf413* causes embryonic lethality. FasII staining of these embryos reveal a range of phenotypes in the central and peripheral motor nerves, featuring axonal growth, pathfinding, branching and misrouting defects. Our findings are important as they implicate a key functional requirement of this gene in precise axonal patterning events, a novel developmental role imparted for an octopamine biosynthesis pathway gene in structuring of embryonic nervous system.

Keywords *Drosophila*, *olf413*, Octopamine, Dopamine, $T\beta H$, Axonal pathfinding, Axonal growth, Nervous system development

Introduction

Neurotransmitters are classical communication molecules extensively studied for their synaptic function mediating transmission. Human and mammalian studies which associate many of the major neurotransmitters to

neurodevelopmental disorders implicate neurotransmitters to have potential roles beyond synaptic communication, in neurodevelopment [1]. The enormous size and complexity of mammalian brain makes it difficult to visualize the developmental deformities at a finer resolution in terms of cellular processes and axonal tracts of neurons. *Drosophila*, which is capable of performing complex activities has a relatively several folds lesser number of neurons in their brain with simpler and definable

*Correspondence:

Baragur Venkatanarayanasetty Shyamala
shyamalabv@yahoo.com

Full list of author information is available at the end of the article



© The Author(s) 2024. **Open Access** This article is licensed under a Creative Commons Attribution 4.0 International License, which permits use, sharing, adaptation, distribution and reproduction in any medium or format, as long as you give appropriate credit to the original author(s) and the source, provide a link to the Creative Commons licence, and indicate if changes were made. The images or other third party material in this article are included in the article's Creative Commons licence, unless indicated otherwise in a credit line to the material. If material is not included in the article's Creative Commons licence and your intended use is not permitted by statutory regulation or exceeds the permitted use, you will need to obtain permission directly from the copyright holder. To view a copy of this licence, visit <http://creativecommons.org/licenses/by/4.0/>. The Creative Commons Public Domain Dedication waiver (<http://creativecommons.org/publicdomain/zero/1.0/>) applies to the data made available in this article, unless otherwise stated in a credit line to the data.

circuits [2]. Further flies as model system offer the most tractable genetic toolkit which enables the analysis of genes for their functions in a context dependent manner [3–8]. Octopamine is a neurotransmitter similar to vertebrate nor adrenaline, controls aggression, sleep, appetite, feeding, courtship etc. in *Drosophila*, as understood through studies on mutants defective for enzyme Tyramine β -Hydroxylase [9]. Here we report an intriguing finding that a paralogous gene *olf413*, predicted to be involved in octopamine biogenesis is essential for developmental patterning of embryonic nervous system.

SG1.1 is a P-*GAL4* enhancer trap strain isolated in our earlier screen for genes with expression in the nervous system [10]. This strain carries single P-*GAL4* insertion on the third chromosome which is homozygous lethal. The strain shows enhancer activity in clusters of neurons in the suboesophageal ganglion (SOG), superior protocerebrum, central brain (CB) region and ventral ganglion (VG) of the adult brain [11, 12]. The expression of the reporter gene in the pupal brain in a temporally regulated cyclical pattern prompted us to characterize the native gene at the site of P-*GAL4* insertion in SG1.1 strain. Here we report the molecular mapping of the P-*GAL4* insertion to 1.9 bp upstream of the transcription start site of the identified native gene *olf413*, as annotated in Berkeley Drosophila Genome Project (BDGP) [13]. The reporter gene expression comparisons and complementation test with a null allele of *olf413* confirmed SG1.1 P-*GAL4* insertion as an allele of *olf413*. Gene *olf413*, annotated as CG12673 has been predicted to code for a protein paralogous to *Tbh* having a role as an enzyme in octopamine biogenesis [14]. Biological function of *olf413* has been very little worked out, except in a few genome-wide association (GWA) screens, food preference and motor behavior analysis [15–19]. This study shows that *olf413* mutants have decreased octopamine levels and the loss of function mutant embryos show severe disruptions in motor nerves of ventral nerve cord (VNC) and their peripheral motor axon projections. Our observations discretely demonstrate in vivo, the critical requirement of *olf413* function in establishing precisely patterned neuronal network during embryonic development.

Methods

Drosophila stocks

The following fly stocks were used: Oregon-K (*Drosophila* Stock Centre, University of Mysore), UAS-*GFP* on III chromosome (National Centre for Biological Sciences, Bengaluru), SG1.1/*TM3Sb* (our lab), Gene disruption strain *olf413*^{MI02014}/*TM3Sb* (#77717, Bloomington *Drosophila* Stock Centre (BDSC)) [20].

Molecular localization of P-*GAL4* insertion

Inverse PCR was carried out using T7 and T3 primers on self-ligated Sac1 and Pst1 digests of SG1.1 genomic DNA. The genomic fragment flanking the P- insertion was sequenced. The flanking genomic sequence mapping was done using Basic Local Alignment Search Tool (BLAST) search against *Drosophila melanogaster* genomic sequence to obtain the precise position of P-*GAL4* insertion.

Lethality test

To decipher the exact stage of lethality in homozygous SG1.1 strain, embryos were collected on 2% sucrose agar medium at 22 °C overnight. 1000 embryos were transferred to 20 vials containing normal wheat cream agar medium with 50 embryos in each vial. The number of live and dead individuals were scored and recorded at each stage (larva, pupa and adult).

To check embryonic lethality, embryos collected were incubated at 25 °C incubator for nearly 48–50 h. The number of unhatched and hatched embryos were tabulated. The unhatched embryos of genotype SG1.1-*GAL4* and *olf413*^{MI02014}, which had completed embryogenesis and were with visible mouth hook were imaged in halocarbon oil under Bright field microscope (ZeissAXIO Imager A2).

Complementation test

Virgin females from SG1.1-*GAL4*/*TM3Sb* were crossed to *olf413*^{MI02014}/*TM3Sb* males, and the F1 progeny embryos were collected and grown as explained in lethality test. The number of F1 adult flies eclosed from 50 × 20 replicates were counted and recorded.

Analysis of reporter gene activity

UAS-*GFP*; SG1.1/*TM3Sb* stock was generated and used for analysis of GFP expression. *olf413*^{MI02014}-*GAL4* virgin females were crossed with UAS-*GFP* (on III chromosome) males, to obtain *olf413*^{MI02014}-*GAL4*/UAS-*GFP* individuals. The embryos collected were dechorionated in 50% sodium hypochlorite solution, rinsed with water, mounted in halocarbon oil and the GFP expression was documented using confocal laser scanning microscope (Zeiss LSM 710). The Z sections were taken at every 1 μ m interval. The 3D projections of Z-Stacks were obtained.

Staged larval and pupal brains were dissected in phosphate buffered saline (PBS) and fixed in 4% paraformaldehyde (PF) fixative in PBS, for 20–30 min at room temperature. The fixed brains were washed in PBS and 0.05% PBTx and mounted in vectashield for imaging.

Immunohistochemistry

15–18 h old embryos selected from an overnight collection of Oregon-K, SG1.1/*TM3Sb* and *olf413^{MI02014}* stocks were analysed. The embryos were dechorionated and fixed in 3.7% formaldehyde in PBS with equal volume of n-heptane (1:1) solution for 20 min, devitalized by 2–3 methanol washes, followed by washes with absolute alcohol. The embryos were rehydrated with grades of alcohol and 0.1% PBTx (1:2, 1:1, 0.1%PBTx) prior to Antibody staining and processed further. Third instar larval brains were dissected in PBS, fixed in 4% PF for 25 min at room temperature, washed with 0.05% PBTx and processed for antibody staining. Antibody staining for both embryos and larval brains was carried out as described in Rohith and Shyamala [21], with minor changes. Primary antibodies used were mouse anti-Fasciclin II (1:10, 1D4, DSHB) for embryos, mouse anti-Repo (DSHB; 1:10) and mouse anti-Elav (DSHB; 1:10) for larval brains. Secondary antibodies used were Goat Anti-Mouse IgG CF™ 488A (1:200; Sigma Aldrich), Goat Alexa fluor 647 anti-mouse IgG (Invitrogen; 1:500). The embryos and brains were mounted in vectashield and imaged with confocal laser scanning microscope (Zeiss LSM 710).

Octopamine quantification

LC–MS/MS analysis was carried out for control (Oregon-K) and mutant (*olf413^{MI02014}* homozygous survivors). 10 heads of just eclosed males and females in equal ratio, were homogenised with 50 µl PBS and 50 µl of 0.1% Formic acid in Acetonitrile (ACN), and centrifuged at 10,000 rpm for 10 min at 5 °C. The supernatant was collected, and stored at – 20 °C until analysis. Octopamine levels were measured with HPLC—Shimadzu LC Prominence 20AT, and Mass Spectrophotometer—AB Sciex, 4000 equipped with a C18, 50*4.6 mm, 4-micron column. The graph represents a mean of three independent experimental replicates for each group.

Statistics

The statistical analysis was performed using SPSS software (Version 22). The octopamine quantity is presented as mean ± SEM. One-way ANOVA and Tukey’s post-hoc honestly significant difference test were applied to compare between the control and mutant groups.

Results

SG1.1 P-GAL4 insertion is an allele of *olf413*

Precise mapping of P-GAL4 insertion in SG1.1 strain was done by Inverse PCR (Methods for details). Two independent restriction digests of SG1.1 genomic DNA using *SacI* and *PstI*, were processed for inverse PCR with T7 and T3 primers (Methods for details). The BLAST search of flanking genomic DNA maps P-GAL4 insertion in this strain to 22,134,168th bp position on the left arm of the 3rd chromosome (79C). This insertion site is 1.9 kb upstream of the transcriptional start site of the annotated gene [13] CG12673 identified as *olf413* (Fig. 1). There are no other annotated protein coding transcripts up to a distance of about 53,370 bases from the site of P-insertion. There is an annotated long non coding RNA—lncRNA-CR45236 at a distance of 12.23 kb upstream of the insertion site whose molecular and biological function are not known. The reporter gene expression pattern as depicted by the expression of UAS-GFP, driven by SG1.1-GAL4 was documented. The embryonic expression pattern of GFP (Fig. 2A) matches with that of the mRNA in situ hybridization pattern for CG12673 [22].

SG1.1 strain has an enhancer activity which covers a subset of expression domains of *olf413* in embryonic and adult nervous system

Lee et al. have generated a gene disruption library of strains which have gene specific T2A-GAL4 insertion in one of the introns of the target gene, thus will be expressed under the endogenous promoter of the gene in question. The transgenic construct also has

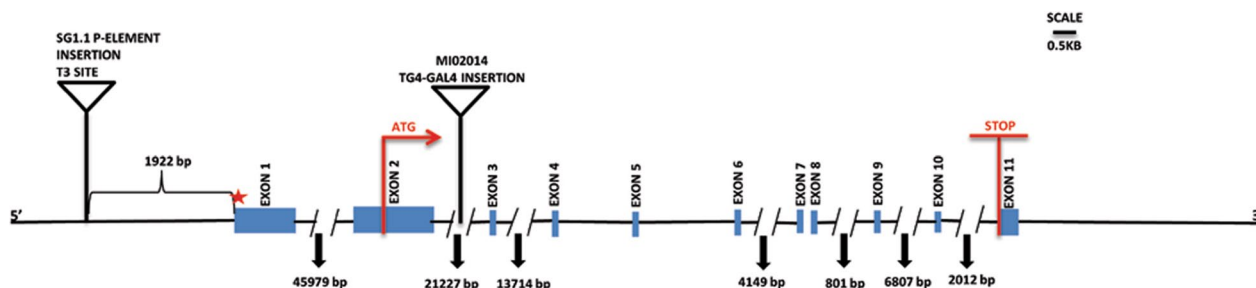


Fig. 1 Mapping of insertion site of P-GAL4 element in *olf413^{SG1.1}* allele of *olf413* gene. The figure depicts the P-GAL4 insertion site in *olf413^{SG1.1}* and the gene disruption strain, *olf413^{MI02014}* on a 5' to 3' directed *olf413* gene span. The rectangular boxes represent the exons. The thin lines indicate the introns. The numbers along each intron represents the length of the respective intron. SG1.1 P-GAL4 element is inserted at 1922 bp upstream of the transcriptional start site of *olf413* (red star). The insertion site of Trojan-GAL4, and the position of start codon (ATG) and Stop codon in *olf413* are marked on the basis of BDGP genome data [13, 20]

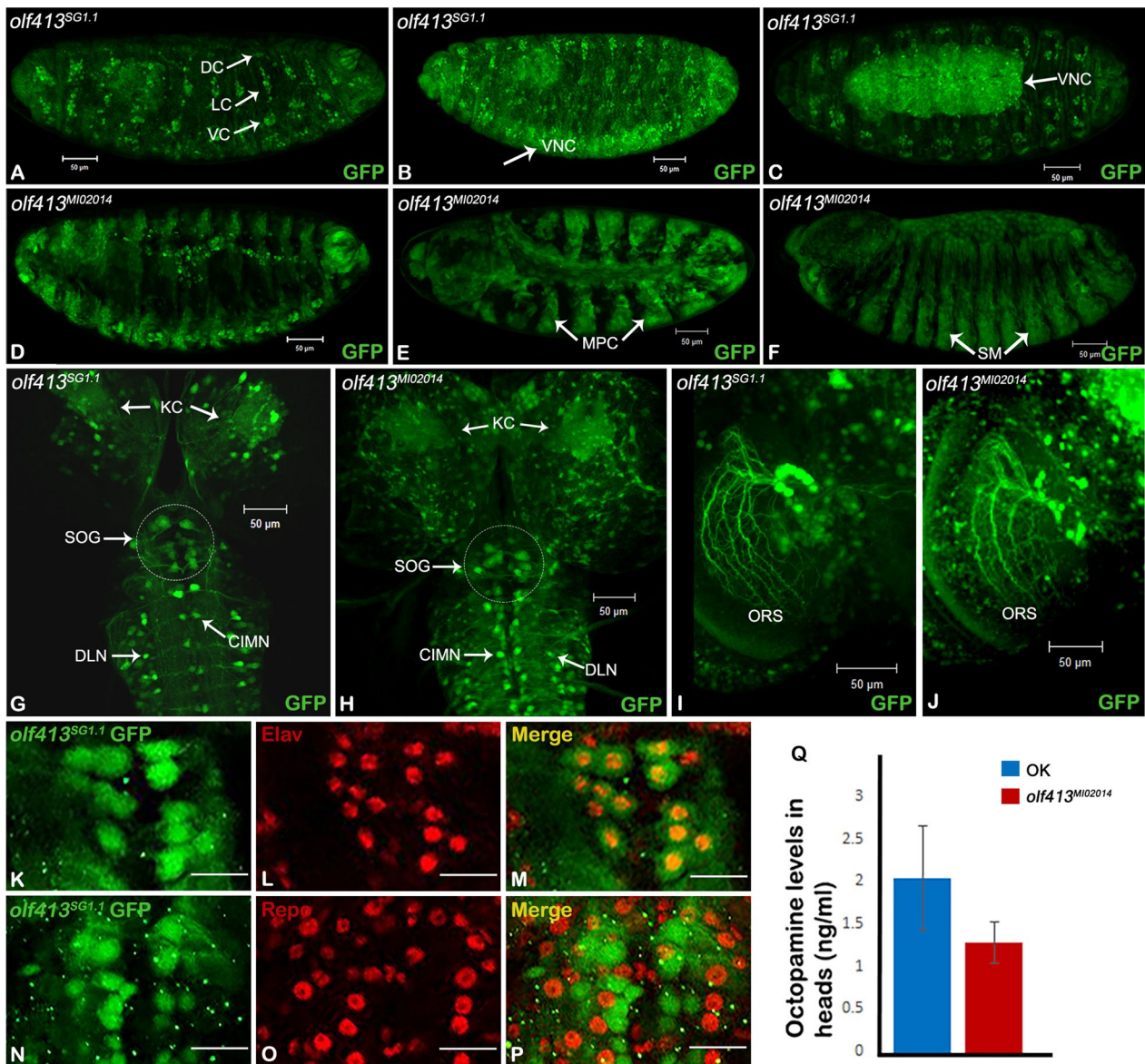


Fig. 2 Enhancer activity pattern in *olf413^{SG1.1}* enhancer trap strain and *olf413^{MIO2014}* as depicted by reporter GFP expression. UAS-GFP strain was crossed with the two *olf413* strains and the reporter GFP expression was analysed. **A** Embryo (stage 16) of *olf413^{SG1.1}* shows an expression in the ventral nerve cord region, in ventral (VC), lateral (LC) and dorsal (DC) neuronal clusters of nervous system. **B** and **C** Stage 12 and stage 17 embryos of *olf413^{SG1.1}* respectively showing the strong expression of GFP in the developing ventral nerve cord (VNC). **D** Stage 16 embryo of *olf413^{MIO2014}*-GAL4/UAS-GFP showing expression pattern similar to *olf413^{SG1.1}*. **E** and **F** Stage 12 and stage 17 embryos of *olf413^{MIO2014}* respectively with a very prominent reporter expression in the somatic muscle precursors (MPC) and Somatic muscle bundles (SM). **G** and **H** 72 h after larval hatched (ALH) (late 3rd instar larva) staged brain of *olf413^{SG1.1}* and *olf413^{MIO2014}* strains respectively shows the reporter gene expression in clusters of neurons in central brain, subesophageal ganglion (SOG) and Kenyon cells (KC). Ventral ganglion has the expression in centrointermediate neurons (CIMN) and the dorsolateral neurons (DLN) of individual segmental neuromeres. **I** and **J** Frontal view of adult brain (101 h APF) of *olf413^{SG1.1}* and *olf413^{MIO2014}* respectively showing lobular plate region. The vertical system neurons of the optomotor responsive system [25] (ORS) shows strong enhanced activity in both the strains. All embryos have anterior to the left and the posterior to the right. **K–M** Brains at 72 h ALH, stained with Anti-Elav antibody (**L**, Red) marked with *olf413^{SG1.1}* GFP (**K**, green). **M** merged image showing that *olf413^{SG1.1}* cells are Elav positive. **N–P** Brains at 72 h ALH stained with Anti-Repo antibody (**O**, Red) and marked with *olf413^{SG1.1}* GFP (**N**, green). **P** merged image showing that *olf413^{SG1.1}* cells do not overlap with Repo positive cells. **Q** Represents the results of LC–MS/MS analysis for octopamine quantification. The bar graphs represent the mean \pm SEM of octopamine levels (n=3) quantified in head samples for homozygous *olf413^{MIO2014}* with Oregon-K as control. **A, B, D, E, F** are lateral views, **C** is ventral view. Scale bar in Fig A–J represents 50 μ m and in (**K–P**) represents 10 μ m

a polyadenylation signal at 3'end of the *GAL4* coding sequence which will arrest transcription following the *GAL4* sequence. Thus it will code for a truncated protein for the target gene, and acts as a null/severe loss of function allele for the gene [20]. *olf413^{MI02014}* is a gene disruption strain from this library which has the T2A-*GAL4* insertion in the second intron after the translational start site for CG12673, the annotated gene for *olf413*. *olf413^{MI02014}* and SG1.1-*GAL4* strains were crossed to UAS-*GFP* and the *GAL4* driven reporter GFP expression was analyzed and compared. The reporter gene expression driven by SG1.1-*GAL4* is seen in the ventral (VC), lateral (LC) and dorsal clusters (DC) of neurons of the peripheral nervous system (PNS) in stage 16 embryo [23] (Fig. 2A). A similar pattern of enhancer activity is seen in *olf413^{MI02014}/UAS-GFP* embryos (Fig. 2D). The two strains share an overall similarity in the pattern of reporter GFP expression in the larval brain (Fig. 2G and H). Clusters of neurons in the central brain, suboesophageal (SOG) and the ventral ganglion are strongly marked while Mushroom body neurons, the kenyon cells (KCs) show faint expression. Segmentally reiterated pairs of neurons along the neuromeres of the VG, which localize to the centroiintermedial (CIMN) and the dorsolateral (DLN) compartments of the fasciclin II (FasII) landmark system [24], express reporter GFP. It is seen that the SG1.1 enhancer activity is restricted to fewer number of neurons as compared to that seen in case of *olf413^{MI02014}* in the respective domains of expression. Figure 2I and J show the lobula plate region of the adult brains of SG1.1/*UAS-GFP* and *olf413^{MI02014}/UAS-GFP* individuals respectively. The dendritic arborization of the vertical system neurons (VS1, VS2, VS3) of the optomotor responsive system (ORS) [25] are strongly marked by the reporter GFP expression. Besides this shared enhancer activity, there are expression patterns which are distinct to the two strains. We see that the embryonic ventral nerve cord in SG1.1-*GAL4* is marked by reporter expression from stage 12, which becomes pronounced by stage 17 (Fig. 2B, C). The endogenous enhancer activity as in *olf413^{MI02014}*, is seen in the developing somatic muscles.

Reporter expression is seen in myoblast clusters of stage 12 embryo, and the dorsal and lateral somatic muscle (SM) bundles of late 17 stage embryo (Fig. 2E, F). This mesodermal specific enhancer activity is not seen in SG1.1-*GAL4* strain. The adult and larval expression patterns of SG1.1-*GAL4* enhancer trap strain recorded during our earlier screening had shown reporter expression restricted to the brain and ventral ganglion of the adult and the larva. Adult and the larval muscles, including other tissues do not show reporter expression [10, 11]. Further to confirm the neural or glial identity of these cells, we have here stained the SG1.1 *GAL4-GFP* larval brains with Anti-Elav (neuronal) and Anti-Repo (glial) marker antibodies. Figure 2K–P depicts the results. We can clearly see that all SG1.1-GFP expressing cells stain positive with anti-Elav antibody (Fig. 2K–M), whereas none of the GFP expressing cells co-localize with anti-Repo antibody (Fig. 2N–P). Thus, demonstrating clearly that, the P-*GAL4* insertion in SG1.1 marks a neuronal specific enhancer of *olf413*.

SG1.1-*GAL4* insertion fails to complement lethality in-trans with *olf413^{MI02014}*

Prompted by the fact that, P-*GAL4* insertion localizes at 1.9 kb upstream of *olf413* transcription start site, and the local enhancer activity pattern maps to a subset of endogenous enhancer activity domains of *olf413*, we subjected the two strains for complementation in-trans test. As mentioned earlier, SG1.1-*GAL4* insertion strain is homozygous lethal at embryonic stage. We checked the gene disruption strain *olf413^{MI02014}* and found that it also shows lethality at embryonic stage with very few escapers (3–4%). The results of the complementation test (Methods) are presented in Table 1. The transheterozygotes SG1.1-*GAL4/olf413^{MI02014}* showed a partial lethality of about 36.4%. This failure in complementation further confirmed that SG1.1-*GAL4* strain is a new allele of *olf413*. And here onwards we denote the strain as *olf413^{SG1.1}* - a new allele of *olf413*.

Table 1 Complementation test- homozygous and in-trans lethality *olf413^{SG1.1}* and *olf413^{MI02014}* alleles

	Control Oregon-K	<i>olf413^{SG1.1}</i> (Homozygous)	<i>olf413^{MI02014}</i> (Homozygous)	<i>olf413^{SG1.1/}</i> <i>olf413^{MI02014}</i>
Number of progeny expected	500	250	100	250
Number of progeny observed	434	0	4	159
% Lethality observed	13.2%	100%*	96%*	36.4%*

The table shows the lethality in percent of homozygotes *olf413^{SG1.1-GAL4}*, homozygotes *olf413^{MI02014}* and transheterozygotes *olf413^{SG1.1/olf413^{MI02014}}* counted as number of non-stubble flies enclosed (complementation test, methods for details) with Oregon-K flies as control

* This lethality was calculated by counting the number of non- stubble flies enclosed

olf413 loss of function mutants show reduced levels of octopamine

Based on the annotated protein product and the identified functional domains, the function of *olf413* gene product is predicted as dopamine beta-monooxygenase, an enzyme in octopamine/ norepinephrine biogenesis. In this context, we wanted to check if octopamine levels are affected in the loss of function mutants of *olf413*. The head samples from *olf413*^{MI02014} homozygous survivor adults were subjected to LC-MS/MS analysis for quantification of octopamine. Three sample runs for each trial set were carried out for the control and the mutant (Methods for details). The results are presented as bar graphs in Fig. 2Q. We find that, in all the trials, the mutant heads consistently showed reduced quantity of octopamine compared to that of the head samples from the control. The results strongly substantiate the predicted function of *olf413* in octopamine biosynthesis.

olf413 loss of function results in severe axonal growth, pathfinding and connectivity defects in embryonic nervous system

The homozygous embryos of *olf413*^{SG1.1} as well as, that of *olf413*^{MI02014} when observed, revealed that they die at very late stage of embryonic development, with the mouth hook and trachea formed (Fig. 3A and B). Intriguingly, some of these embryos showed wriggling movements within the chorion and made attempts to hatch out, but failed to move out of the chorion. This observation was strongly indicative of a probable problem with the neuromuscular coordination and disability. Fasciclin II antibodies provide an effective tool to identify motor axon defects. We stained the late staged (16–17 stage) homozygous embryos with Anti-FasII antibody. The

results are presented in Fig. 3C–S. Figure 3C and D represent wild type ventral nerve cord and peripheral motor nerves pattern. The *olf413*^{SG1.1} homozygous embryos showed grades of deformities in the longitudinal tracts of the ventral nerve cord and the peripheral motor nerves (Fig. 3E–I). Most severe phenotypes with an occurrence of 40% had highly disorganized ventral nerve cord and the peripheral motor projections (Fig. 3E). Embryos with moderate phenotypes had breaks in the VNC, axonal growth defects, disordered and misrouted axons evading segmental boundaries (Fig. 3F and G). The milder phenotypes presented frequent midline crossing of the longitudinal tracts (Fig. 3H). The enlarged views highlight these defects in detail (Fig. 3E'–H'). The inter segmental (ISN) and segmental (SN) motor projection neurons showed defects like fusion of ISN and SN nerves into single tract, misrouting of axons to cross the segmental boundaries. Excessive and abnormal branching, premature termination of growth before they reach their respective target muscles were commonly seen among motor axon projections (Fig. 3I).

The VNC and peripheral motor projection axon phenotypes seen in homozygous embryos of *olf413*^{MI02014} strain were relatively much more severe (Fig. 3J–N). This was expected as loss of function of *olf413* in this case is both in the neurons as well as in the somatic muscles. Highly disordered and messed up VNC with stunted and misrouted projection nerves featured the phenotypes with an occurrence of 56.2% (Fig. 3J–M). Detailed view of these defects are seen in Fig. 3J'–M'. Multiple defects found in peripheral motor projection nerves were comparable to that seen in *olf413*^{SG1.1} homozygotes (Fig. 3N). In summary, the phenotype observed demonstrates that the function of *olf413* is critically

(See figure on next page.)

Fig. 3 Central and peripheral motor neuron axon guidance defects in mutant *olf413*^{SG1.1}, *olf413*^{MI02014} and trans-heterozygotes *olf413*^{SG1.1/olf413}^{MI02014} embryos. **A** and **B** The bright field images of lethal embryos of *olf413*^{SG1.1} and *olf413*^{MI02014} homozygotes respectively showing the mouth hook (MH) and trachea (TR) completely formed (green arrows). **C–S** Embryos at stage 16–17 stained with Anti-Fasciclin II antibody (mAB-1D4) to label the axonal tracts of both ventral nerve cord and peripheral nerves. **C** and **D** are the Oregon-K embryos of stage 16–17, showing the wild type VNC and the peripheral motor nerves (PMN) respectively. The inter-segmental nerve (ISN) and segmental nerve (SN) are marked with white arrows. **E–I** Represent the VNC and the PMN of *olf413*^{SG1.1} homozygotes. **E** Most severe VNC and PNS deformities. **F** and **G** Moderate phenotype with axonal growth defect in VNC, disrupted and misrouted PMN. **H** Midline crossing of longitudinal tracts. **E'–H'** Enlarged view of marked region in (**E–H**). **I** Lateral view of peripheral projection nerves showing different growth and pathfinding defects. **J–N** Represent the VNC and PMN of *olf413*^{MI02014} homozygotes. **J–M** Most severe VNC and PNS deformities. **J'–M'** Enlarged view of marked region in (**J–M**). **N** Lateral view of peripheral projection nerves showing severe growth and pathfinding defects. **O–S** Represent the VNC and PMN of *olf413*^{SG1.1/olf413}^{MI02014} transheterozygotes. **O** Most severe VNC and PNS deformities. **P** and **Q** moderate growth and pathfinding defects. **R** Mid line crossing of longitudinal tracts. **O'–R'** Enlarged view of marked region in (**O–R**). **S** Lateral view of peripheral projection nerves showing different growth and pathfinding defects. In all figures, arrows indicate breaks in VNC (red), axonal thinning and growth defect (purple), disordered or misrouted axons evading segmental boundaries (blue), and midline crossing of the longitudinal tracts (yellow). The peripheral motor projection defects are indicated by arrowheads- premature termination of growth, asterisks- fusion or fasciculation of ISN and SN into one nerve, rhomboid- excessive or abnormal branching of axons, star- misrouting of axons extending across the segmental boundaries, where the ISN of one segment fasciculate with the nearby ISN segment, and white arrow- de-fasciculation or branching at the ends of ISN. In the images showing VNC, the embryos are positioned with anterior to the top, whereas for the embryos showing PMN, they are positioned with anterior to the left. Scale bar represents 50 μm

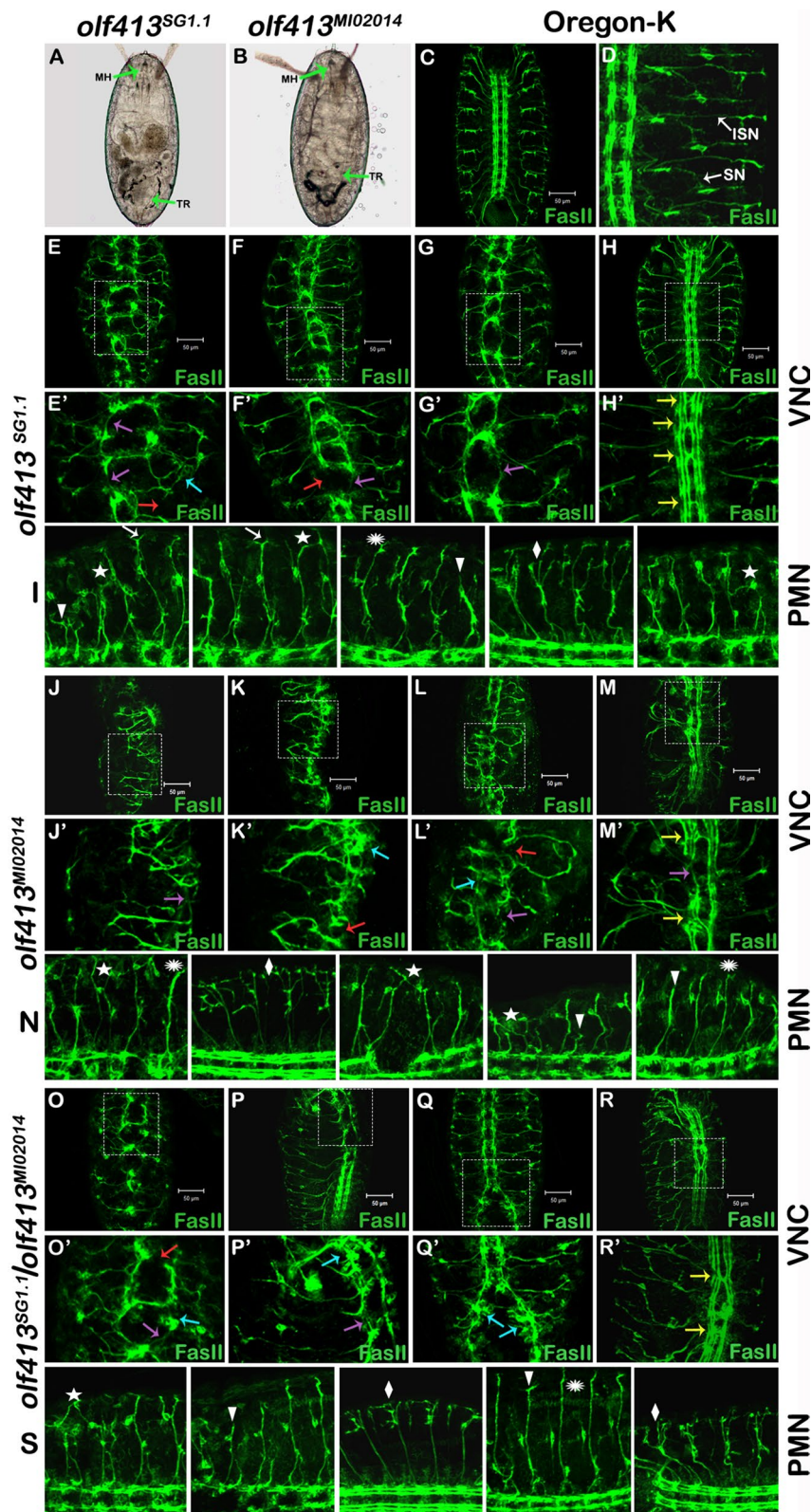


Fig. 3 (See legend on previous page.)

required for proper axonal growth, guidance, branching and target connectivity in both the VNC and peripheral motor projections during embryonic development. The transheterozygote *olf413^{SG1.1}/olf413^{MI02014}* embryos stained with Anti-FasII antibodies showed similar range of longitudinal tract and motor axon pathfinding defects (Fig. 3O–R). The frequency of occurrence of the most severe phenotypes was 46.15%. Figure 3O'–R' show enlarged views of the VNC defects. Figure 3S depicts various peripheral motor projection defects observed. All the axonal tract defects seen in the *olf413^{SG1.1}* and *olf413^{MI02014}* homozygotes were also seen in the transheterozygotes, though represented in lesser number of embryos. These results imply that the two strains fail to complement each other with respect to the axonal tract defects as well.

Discussion

SG1.1, a P-GAL4 strain was studied in detail for its molecular localization, enhancer activity pattern and genetic complementation with a putative candidate native gene *olf413*. Our experiments demonstrated that SG1.1-GAL4 strain is a neuronal specific allele of *olf413* (CG12673). *olf413* has been annotated as a protein coding gene with predicted copper type II ascorbate-dependent monooxygenase domain, tyramine/dopamine beta-hydroxylase signature domains [26]. The biological functions of *olf413* have been little studied. It has been identified as an associated gene in a few GWA analysis studies carried out for psychostimulant drug preferences [15] and dietary dependent reduction in life span and starvation resistance [16, 17]. Recently studies have shown food preference, feeding and motor activity defects in *olf413* mutant adults [18, 19].

In the present study, we have used the gene disruption strain *olf413^{MI02014}* in conjunction with *olf413^{SG1.1}* to describe for the first time, the detailed expression pattern and role of the gene *olf413* in embryonic development and octopamine biogenesis. Our finding that the homozygous mutants show a decreased level of octopamine, strongly agrees with the predicted function of the gene in octopamine biogenesis. Analysis of lethal homozygous (*olf413^{SG1.1}*, *olf413^{MI02014}*) and transheterozygote (*olf413^{SG1.1}/olf413^{MI02014}*) by Anti-FasII antibody staining has revealed extremely severe to mild deformities in the embryonic ventral nerve cord and peripheral motor projection nerves. Relatively more distorted VNC and peripheral axonal phenotypes in *olf413^{MI02014}* embryos indicate that, the neuronal, as well as the muscle specific expression of the gene are required, and function in synergy with each other to facilitate axon growth and guidance to establish precise patterning of the neuronal tracts during embryonic development.

By DRSC integrative ortholog prediction tool (DIOPT) reports [27], *olf413* has been identified as a paralogue of *TβH* gene which codes for Tyramine β Hydroxylase, a key enzyme in octopamine biosynthesis pathway [28, 29]. Octopamine being a neurotransmitter and neuromodulator [30, 31] *TβH* null mutants which suffer octopamine deficits have been assayed for various behavioural phenotypes. TβH function has been implied in regulating aggression [32], courtship [33], sleep behavior [34], learning and memory [35], dietary response [36, 37] larval locomotion [38] and Tau pathogenicity in flies [39]. Nevertheless, so far in vivo embryonic expression and embryonic mutant phenotypes imparting a developmental role, have not been demonstrated for *TβH*. *TβH* null flies survive till adulthood with normal morphology but exhibit ovulation defect [14, 40]. While orthologous genes typically perform equivalent functions, paralogues in general evolve through subfunctionalization and subsequent neofunctionalization [41]. Here we have shown that *olf413*, a paralogue of *TβH*, has been deployed to perform a distinct role in the development of embryonic nervous system. Developmental role for neurotransmitters has long been implicated in Humans and other mammalian systems [1]. Studies have been carried out through pharmacological interventions using receptor blockers and antagonists in mammalian models for major neurotransmitters like serotonin [42–45], norepinephrine [46], dopamine [47], GABA [48, 49] and acetylcholine [50]. Genetic studies in Humans include classical chromosomal aberrations associations, and genome-wide association studies (GWAS) relating neurotransmitters to neurodevelopmental diseases [51, 52]. The probable structural connectivity disturbances in these studies have been suggested based on the behavioral and cognitive impairments and altered electrical recordings observed in the subjects. A few in vitro cell culture studies have shown that neurotransmitters administered in culture modulate axon growth and branching. [53, 54]. These studies show indirectly the non-synaptic, developmental roles of neurotransmitters in mammalian brain. The relative simplicity of the cellular content and the neuronal circuitry in *Drosophila* nervous system has allowed us to demonstrate in this study for the first time, the functional requirement of an octopamine biosynthesis pathway gene for precise axonal growth, and patterning during embryonic development at a finer resolution in vivo.

Limitations

We have demonstrated the critical requirement of *olf413* for embryonic nervous system development and biosynthesis of neurotransmitter octopamine. But further qPCR and immunohistochemical quantification

experiments are needed to be carried out to demonstrate if the *olf413* transcript and protein levels are affected in the mutants studied.

Abbreviations

SOG	Suboesophageal ganglion
CB	Central brain
VG	Ventral ganglion
BDGP	Berkeley Drosophila Genome Project
TβH	Tyramine β hydroxylase
GWA	Genome-wide association
VNC	Ventral nerve cord
BDSC	Bloomington Drosophila Stock Centre
BLAST	Basic Local Alignment Search Tool
VC	Ventral clusters
LC	Lateral clusters
DC	Dorsal clusters
PNS	Peripheral nervous system
KCs	Kenyon cells
CIMN	Centrointermedial neurons
DLN	Dorsolateral neurons
VS	Vertical system neurons
ORS	Optomotor responsive system
SM	Somatic muscle
MPC	Muscle precursor cells
FasII	Fasciclin II
ISN	Inter segmental neurons
SN	Segmental neurons
MH	Mouth hook
TR	Trachea
DIOPT	DRSC integrative ortholog prediction tool
DSHB	Developmental Studies Hybridoma Bank

Acknowledgements

We thank *Drosophila* stock center, Mysuru; National Center for Biological Sciences, Bengaluru; Dr. Gurudata V Baraka, Center for Human Genetics, Bangalore; Bloomington Drosophila Stock Center, USA; for the fly stocks. We thank DSHB, USA for the antibodies. We are thankful to the Institute of Excellence, University of Mysore, Mysuru and National Center for Biological Sciences, Bengaluru, for providing confocal and bright field imaging facility. We acknowledge the support of Dr. B.N. Rohith in confocal microscopy.

Author contributions

BVS conceived and designed the study. CRV carried out the molecular localization experiments and did data analysis. RR carried out the expression studies immunohistochemistry and mutant analysis experiments. BVS and RR and CRV made interpretations of the data. RR prepared the Figs. 1, 2, 3. BVS and RR prepared the manuscript with contributions from all the authors, and are involved in critically reviewing and revising the analysis and interpretations. All the authors have read and approved the final manuscript.

Funding

RR was supported by funds from Institute of Excellence, Project fellowship, University of Mysore, Mysuru, Karnataka, India (UOM/IOE/Project fellow 699/2019-20 Dt: 01/01/2020). Research was supported by funds from University of Mysore CAS-SAP funds, (DV4/228/UGC-CAS-1/2015-2016).

Availability of data and materials

Data available on request from the corresponding author.

Declarations

Ethics approval and consent to participate

Not applicable.

Consent for publication

Not applicable.

Competing interests

The authors declare that they have no competing interests.

Author details

¹Developmental Genetics Laboratory, Department of Studies in Zoology, University of Mysore, Mysuru 570006, India.

Received: 12 April 2023 Accepted: 23 January 2024

Published online: 07 February 2024

References

- Kolk SM, Rakic P. Development of prefrontal cortex. *Neuropsychopharmacology*. 2022;47(1):41–57.
- Kasture AS, Hummel T, Susic S, Freissmuth M. Big lessons from tiny flies: *Drosophila melanogaster* as a model to explore dysfunction of dopaminergic and serotonergic neurotransmitter systems. *Int J Mol Sci*. 2018;19(6):1788.
- O’Kane CJ, Gehring WJ. Detection in situ of genomic regulatory elements in *Drosophila*. *Proc Natl Acad Sci USA*. 1987;84(24):9123–7.
- Wilson C, Pearson RK, Bellen HJ, O’Kane CJ, Grossniklaus U, Gehring WJ. P-element-mediated enhancer detection: an efficient method for isolating and characterizing developmentally regulated genes in *Drosophila*. *Genes Dev*. 1989;3(9):1301–13.
- Brand AH, Perrimon N. Targeted gene expression as a means of altering cell fates and generating dominant phenotypes. *Development*. 1993;118(2):401–15.
- Kennerdell JR, Carthew RW. Use of dsRNA-mediated genetic interference to demonstrate that frizzled and frizzled 2 act in the wingless pathway. *Cell*. 1998;95:1017–26.
- Perkins LA, Holderbaum L, Tao R, Hu Y, Sopko R, McCall K, et al. The transgenic RNAi project at Harvard Medical School: resources and validation. *Genetics*. 2015;201(3):843–52.
- Bassett AR, Tibbit C, Ponting CP, Liu JL. Highly efficient targeted mutagenesis of *Drosophila* with the CRISPR/Cas9 system. *Cell Rep*. 2013;4:220–8.
- Tyramine beta hydroxylase, *InteractiveFly*: GeneBrief, Society for Developmental Biology. <https://www.sdbonline.org/sites/fly/genebrief/tyraminebetahyd.htm>, Accessed 10 Nov 2023.
- Shyamala BV, Chopra A. *Drosophila melanogaster* chemosensory and muscle development: Identification and properties of a novel allele of scalloped and of a new locus, SG18.1, in a Gal4 enhancer trap screen. *J Genet*. 1999;78:87.
- Venkatesh CR, Shyamala BV. Developmentally regulated expression of reporter gene in adult brain specific GAL4 enhancer traps of *Drosophila melanogaster*. *J Genet*. 2010;20:1–6.
- Venkatesh CR, Shyamala BV. GAL4 enhancer trap strains with reporter gene expression during the development of adult brain in *Drosophila melanogaster*. *J Genet*. 2010;89(4):e38–42.
- Adams MD, Celniker SE, Holt RA, Evans CA, Gocayne JD, Amanatides PG, et al. The genome sequence of *Drosophila melanogaster*. *Science*. 2000;287(5461):2185–95.
- Monastiriotti M, Linn CE, White K. Characterization of *Drosophila tyramine β-hydroxylase* gene and isolation of mutant flies lacking octopamine. *J Neurosci*. 1996;16:3900–11.
- Highfill CA, Baker BM, Stevens SD, Anholt RRH, Mackay TFC. Genetics of cocaine and methamphetamine consumption and preference in *Drosophila melanogaster*. *PLoS Genet*. 2019;15(5): e1007834.
- Huang W, Campbell T, Carbone MA, Jones WE, Unselt D, Anholt RRH, Mackay TFC. Context-dependent genetic architecture of *Drosophila* life span. *PLoS Biol*. 2020;18(3): e3000645.
- Patel SP, Talbert ME. Identification of genetic modifiers of lifespan on a high sugar diet in the *Drosophila* Genetic Reference Panel. *Heliyon*. 2021;7(6): e07153.
- Ramya R, Shyamala BV. *olf413* gene controls taste recognition, preference and feeding activity in *Drosophila melanogaster*. *Annu Res Rev Biol*. 2023;38(5):24–31.
- Ramya R, Shyamala BV. *olf413*, a putative octopamine biosynthesis pathway gene is required for negative geotactic motor function in *Drosophila melanogaster*. *J Genet*. 2023;102:52.

20. Lee PT, Zirin J, Kanca O, Lin WW, Schulze KL, Li-Kroeger D, et al. A gene-specific *T2A-GAL4* library for *Drosophila*. *Elife*. 2018;7: e35574.
21. Rohith BN, Shyamala BV. Scalloped a member of the Hippo tumor suppressor pathway controls mushroom body size in *Drosophila* brain by non-canonical regulation of neuroblast proliferation. *Dev Biol*. 2017;432(2):203–14.
22. Fisher B, Weiszmänn R, Frise E, Hammonds A, Tomancak P, Beaton A, et al. BDGP insitu homepage. Patterns of gene expression in *Drosophila* embryogenesis. 2012. <https://flybase.org/reports/FBRef0219073.html>. Accessed 10 Nov 2023.
23. Campos-Ortega JA, Hartenstein V. Stages of *Drosophila* embryogenesis. In: Campos-Ortega JA, Hartenstein V, editors. The embryonic development of *Drosophila melanogaster*. Berlin: Springer; 1985. p. 84.
24. Vömel M, Wegener C. Neuroarchitecture of aminergic systems in the larval ventral ganglion of *Drosophila melanogaster*. *PLoS ONE*. 2008;3(3): e1848.
25. Rajashekhar KP, Shamprasad VR. Golgi analysis of tangential neurons in the lobula plate of *Drosophila melanogaster*. *J Biosci*. 2004;29(1):93–104.
26. Gaudet P, Livstone MS, Lewis SE, Thomas PD. Phylogenetic-based propagation of functional annotations within the Gene Ontology consortium. *Brief Bioinform*. 2011;12(5):449–62.
27. Hu Y, Flockhart I, Vinayagam A, Bergwitz C, Berger B, Perrimon N, Mohr SE. An integrative approach to ortholog prediction for disease-focused and other functional studies. *BMC Bioinform*. 2011;12:357.
28. Livingstone MS, Tempel BL. Genetic dissection of monoamine neurotransmitter synthesis in *Drosophila*. *Nature*. 1983;303(5912):67–70.
29. Wallace BG. The biosynthesis of octopamine—characterization of lobster tyramine beta-hydroxylase. *J Neurochem*. 1976;26(4):761–70.
30. Evans PD. Octopamine. In: Kerkut GA, Gilbert LI, editors. *Comprehensive insect physiology, biochemistry and pharmacology*. Oxford: Pergamon; 1985. p. 499–530.
31. David JC, Coulon JF. Octopamine in invertebrates and vertebrates: a review. *Prog Neurobiol*. 1985;24(2):141–85.
32. Hoyer SC, Eckart A, Herrel A, Zars T, Fischer SA, Hardie SL, Heisenberg M. Octopamine in male aggression of *Drosophila*. *Curr Biol*. 2008;18(3):159–67.
33. Certel SJ, Savella MG, Schlegel DC, Kravitz EA. Modulation of *Drosophila* male behavioral choice. *Proc Natl Acad Sci*. 2007;104:4706–11.
34. Crocker A, Sehgal A. Octopamine regulates sleep in *Drosophila* through protein kinase A-dependent mechanisms. *J Neurosci*. 2008;28(38):9377–85.
35. Iliadi KG, Iliadi N, Boulianne GL. *Drosophila* mutants lacking octopamine exhibit impairment in aversive olfactory associative learning. *Eur J Neurosci*. 2017;46(5):2080–7.
36. Schützler N, Girwert C, Hugli I, Mohana G, Roignant JY, Ryglewski S, Duch C. Tyramine action on motoneuron excitability and adaptable tyramine/octopamine ratios adjust *Drosophila* locomotion to nutritional state. *Proc Natl Acad Sci USA*. 2019;116(9):3805–10.
37. Damrau C, Toshima N, Tanimura T, Brembs B, Colomb J. Octopamine and tyramine contribute separately to the counter-regulatory response to sugar deficit in *Drosophila*. *Front Syst Neurosci*. 2018;11:100.
38. Fox LE, Soll DR, Wu CF. Coordination and modulation of locomotion pattern generators in *Drosophila* larvae: effects of altered biogenic amine levels by the tyramine β hydroxylase mutation. *J Neurosci*. 2006;26:1486–98.
39. Nangia V, O'Connell J, Chopra K, Qing Y, Reppert C, Chai CM, Bhasin K, Colodner KJ. Genetic reduction of tyramine β hydroxylase suppresses Tau toxicity in a *Drosophila* model of tauopathy. *Neurosci Lett*. 2021;755:135937.
40. Monastiriotti M. Distinct octopamine cell population residing in the CNS abdominal ganglion controls ovulation in *Drosophila melanogaster*. *Dev Biol*. 2003;264:38–49.
41. Koonin EV. Orthologs, paralogs, and evolutionary genomics. *Annu Rev Genet*. 2005;39:309–38.
42. Gaspar P, Cases O, Maroteaux L. The developmental role of serotonin: news from mouse molecular genetics. *Nat Rev Neurosci*. 2003;4:1002–12.
43. Trowbridge S, Narboux-Neme N, Gaspar P. Genetic models of serotonin (5-HT) depletion: what do they tell us about the developmental role of 5-HT? *Anat Rec*. 2011;294:1615–23.
44. Kinast K, Peeters D, Kolk SM, Schubert D, Homberg JR. Genetic and pharmacological manipulations of the serotonergic system in early life: neurodevelopmental underpinnings of autism-related behavior. *Front Cell Neurosci*. 2013;7:72.
45. Garcia LP, Witteveen JS, Middelma A, van Hulten JA, Martens GJM, Homberg JR, et al. Perturbed developmental serotonin signaling affects prefrontal catecholaminergic innervation and cortical integrity. *Mol Neurobiol*. 2019;56:1405–20.
46. Saboory E, Ghasemi M, Mehranfard N. Norepinephrine, neurodevelopment and behavior. *Neurochem Int*. 2020;135:104706.
47. Money KM, Stanwood GD. Developmental origins of brain disorders: roles for dopamine. *Front Cell Neurosci*. 2013;7:260.
48. Ben-Ari Y. Excitatory actions of GABA during development: the nature of the nurture. *Nat Rev Neurosci*. 2002;3:728–39.
49. Wang DD, Kriegstein AR. Defining the role of GABA in cortical development. *J Physiol*. 2009;587:1873–9.
50. Janiesch PC, Kruger HS, Poschel B, Hanganu-Opatz IL. Cholinergic control in developing prefrontal-hippocampal networks. *J Neurosci*. 2011;31:17955–70.
51. Marin-Padilla M. Structural abnormalities of the cerebral cortex in human chromosomal aberrations: a Golgi study. *Brain Res*. 1972;44:625–9.
52. Niemi MEK, Martin HC, Rice DL, Gallone G, Gordon S, Kelemen M, et al. Common genetic variants contribute to risk of rare severe neurodevelopmental disorders. *Nature*. 2018;562:268–71.
53. Torráo AS, Britto LR. Neurotransmitter regulation of neural development: acetylcholine and nicotinic receptors. *An Acad Bras Cienc*. 2002;74(3):453–61.
54. Ojeda J, Ávila A. Early actions of neurotransmitters during cortex development and maturation of reprogrammed neurons. *Front Synaptic Neurosci*. 2019;21(11):33.

Publisher's Note

Springer Nature remains neutral with regard to jurisdictional claims in published maps and institutional affiliations.